Science Bulletin 70 (2025) 1523–1532

Contents lists available at ScienceDirect

Science Bulletin

journal homepage: www.elsevier.com/locate/scib

www.scibull.com

Article

Abrupt loss of species richness caused by ecosystem transition

Li Fu [a], Jianping Huang [a,b,*], Guolong Zhang [b], Dongliang Han [b], Lei Ding [a], Yun Wei [c], Xiaoyue Liu [a], Changyu Li [b], Haipeng Yu [d]

[a] *Key Laboratory for Semi-Arid Climate Change of the Ministry of Education, College of Atmospheric Sciences, Lanzhou University, Lanzhou 730000, China*
[b] *Collaborative Innovation Center for Western Ecological Safety, Lanzhou University, Lanzhou 730000, China*
[c] *Department of Atmospheric Science, School of Environmental Studies, China University of Geosciences, Wuhan 430074, China*
[d] *Key Laboratory of Cryospheric Science and Frozen Soil Engineering, Nagqu Plateau Climate and Environment Observation and Research Station of Xizang Autonomous Region, Northwest Institute of Eco-Environment and Resources, Chinese Academy of Sciences, Lanzhou 730000, China*

ARTICLE INFO

Article history:
Received 29 March 2024
Received in revised form 26 November 2024
Accepted 27 November 2024
Available online 3 March 2025

Keywords:
Ecosystem transition
Species richness loss
Abrupt change
Climate change

ABSTRACT

Ecosystem transition occurs when ecological thresholds are crossed, causing ecosystems to irreversibly shift from secure to insecure states. However, how ecosystem transition exacerbates species richness loss remains poorly understood. This hinders the effective protection of species richness, which is an urgent global priority. In this study, we integrated multiple ecosystem variables to elucidate ecosystem transition and its impacts on species richness loss. Our findings reveal that species richness declines abruptly following ecosystem transition, as insecure ecosystems are characterized by reduced plant cover and productivity, intensified warming and drying, and diminished oxygen production. Insecure ecosystems imperil the survival of all species, including 39.4% of threatened birds and 29.2% of threatened mammal species. We project that by 2100, the ecosystem areas considered insecure will encompass 40.4% of the global land areas under the RCP8.5 scenario, contributing to 51.6% of species richness loss. In contrast, hyper-secure ecosystems are projected to account for 18.1% of species richness loss. This study identifies ecosystem transition as a critical driver of species richness loss that should be accounted for by policymakers in designing targeted conservation strategies.

1. Introduction

Climate change is driving substantial changes in ecosystem attributes and functions, exerting widespread and far-reaching impacts on life on Earth [1]. The escalating frequency of climate crises, such as global warming, glacier melting, drought, and heatwaves [2–4], combined with unsustainable human activities like overconsumption of fossil fuels [5] and terrestrial water storage depletion [6], is destabilizing the natural balance of ecosystems at an alarming pace. Of particular concern is that ecosystem changes may occur abruptly once certain environmental thresholds are exceeded [7]. Building upon ecological theories, including regime shifts [8], tipping points [9], and alternative stable states [10,11], we propose the concept of "ecosystem transition", which refers to the shift of ecosystems from secure to insecure states driven by multiple ecosystem variables. Such a transition is triggered by positive feedback when ecological thresholds are crossed, resulting in a new equilibrium state.

Recent studies have identified critical thresholds in various ecological processes, indicating how ecosystems respond to environmental changes. For example, temperature thresholds are associated with the sensitivity of ecosystem respiration [12], which exhibits an unimodal response [13]. Soil moisture thresholds influence plant water stress in terrestrial ecosystems [14] and have been shown to affect soil biodiversity and functions when specific water availability thresholds are crossed [15]. Aridity thresholds significantly alter nitrogen cycling in arid and semi-arid grasslands [16]. Furthermore, several studies have investigated transitions triggered by threshold crossings, focusing on boreal biomes [17], tropical forests [18], and dryland ecosystems [7]. Although these works are invaluable for understanding ecological thresholds, their focus on single factors or specific regions constrains our ability to capture the complexity of ecosystems influenced by multiple factors. To address this, we integrated 19 ecosystem variables to elucidate ecosystem transition and provide a comprehensive assessment of their interactions.

Species richness is a key indicator of ecosystem health and stability, and ecosystem transition profoundly impacts species diversity. Currently, tens of thousands of species are threatened with extinction, raising significant global concern [19,20]. According to

---

* Corresponding author.
E-mail address: hjp@lzu.edu.cn (J. Huang).

https://doi.org/10.1016/j.scib.2025.03.001
2095-9273/

the WWF's Living Planet Report 2022, wildlife populations declined by an average of 69% between 1970 and 2018 [21]. Studies have indicated climate change [22], abrupt land-use changes [23,24], habitat loss, and fragmentation [25] as primary drivers of biodiversity loss. Moreover, overhunting [26] and overfishing [27] have significantly contributed to species population declines. Together, these factors underscore the escalating and multifaceted nature of the global biodiversity crisis. Projections suggest that biodiversity loss will continue to intensify, with extinction risks threatening up to one in six species as a result of future global warming [22]. A recent report emphasizes that the climate and biodiversity crises must be tackled simultaneously, serving as a reminder that failure to mitigate climate change will significantly accelerate species richness loss [28]. This alarming situation has prompted biologists to warn of an impending sixth mass extinction [29], highlighting the urgent need for species conservation. Despite extensive research focused on biodiversity loss, interactions among multiple ecosystem variables and their collective impact on species richness loss remain underexplored. Given the severity of the situation, our study provides new insights into species richness loss driven by ecosystem transition. It offers a scientific basis for policymakers to identify early warning signals of species decline and develop targeted conservation strategies.

In this study, we analyzed the response of 19 ecosystem variables, representing abiotic and biotic characteristics of ecosystems, to the ecosystem security index (ESI) [7,30,31]. To test the hypothesis regarding the threshold of ecosystem transition, we employed threshold regression models and cluster analysis [7,15] (Fig. 1). Our goal is to classify ecosystems into two states, "secure" and "insecure", each with two levels. We then examined the impact of ecosystem transition on threatened species and projected future species richness loss. Subsequently, we elucidated how key ecosystem variables directly or indirectly influence threatened bird and mammal species (Fig. S1 online).

2. Data and methods

2.1. Data

The inherent complexity and dynamics of ecosystems necessitate a multifaceted approach to accurately assess changes, as reliance on a single variable is insufficient. We selected a set of important and commonly used variables to identify ecosystem transition (Table 1). Data on threatened birds and mammals were derived from Jenkins [32]. The future projections of the net change in local species richness since 1500 under RCP8.5 and RCP4.5 scenarios were provided by Newbold [23]. Additional detailed descriptions of datasets are provided in the Supplementary materials.

2.2. Ecological security index (ESI)

Ecosystems are complex systems consisting of biogeochemical cycles including oxygen, carbon, water, heat, and biological processes, all of which are essential for sustaining vegetation, animal

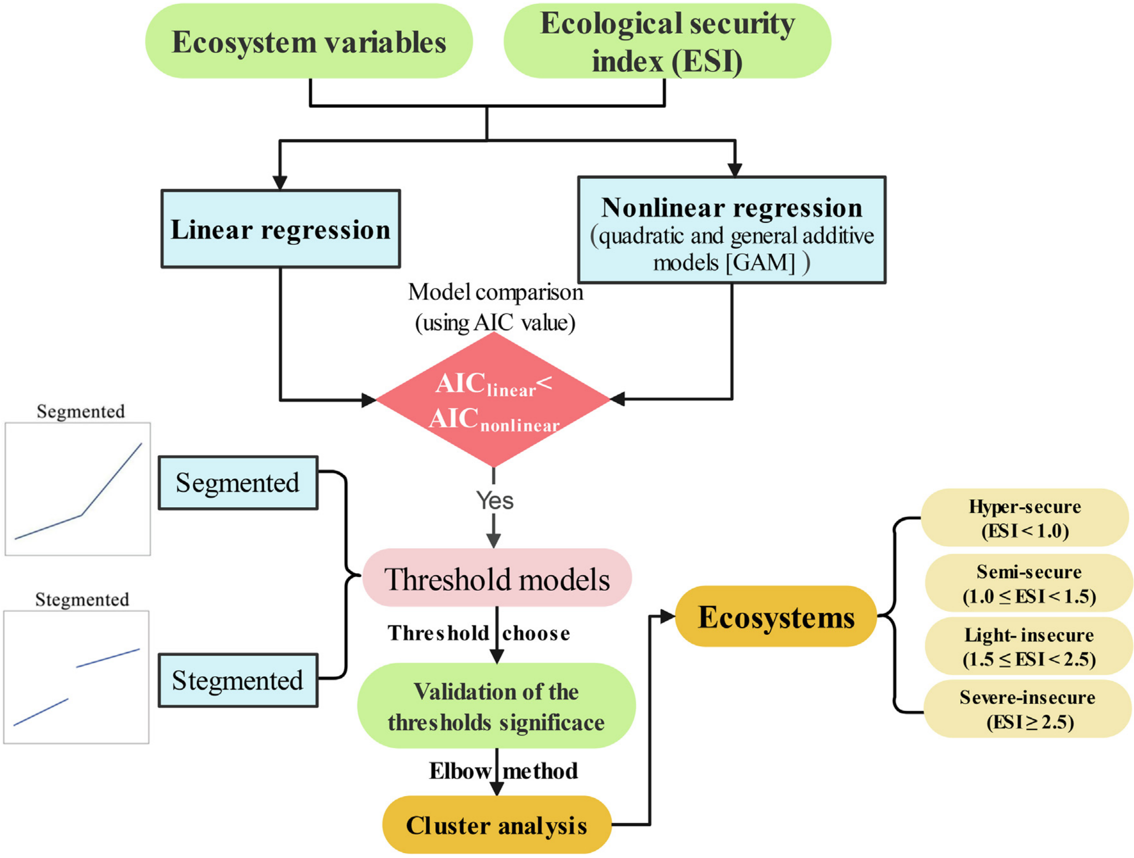

Fig. 1. Workflow for detecting thresholds of ecosystem transition.

Table 1
19 ecosystem variables used in this study.

Database type	Description / Abbreviation			
Climate data	Sensible heat flux (Hs) Evapotranspiration (Evap)	Latent heat flux (LE)	Temperature	Precipitation
Soil data	Soil moisture	Soil temperature	Soil biodiversity index (Soilbio)	Soil pH
	Sand content	Total nitrogen (TN)	Organic carbon (OC)	
Vegetation data	Vegetation sensitivity index (VSI)	Net primary production (NPP)	Normalized difference vegetation index (NDVI)	Leaf area index (LAI)
Human activity data	Human footprint	Human development index (HDI)	GDP per capita (GDP_per)	

life, and human well-being (Fig. S2 online) [33]. Based on this, the study adopted the ecological security index (ESI), developed by Huang et al. [34], which integrates the aforementioned five cycles to comprehensively assess terrestrial ecosystem states. The ESI is defined as:

$$ESI = \left(\frac{O_c}{O_p} \cdot T_m \cdot \frac{1}{AI}\right)^{1/3} \times 10$$

where the parameters Oc and Op represent the consumption and production of oxygen, respectively; the Tm is the temperature warming magnification, and AI is the aridity index. Detailed descriptions of each term are provided in the Supplementary materials (Fig. S3 online).

2.3. Detection and classification of ecosystem transition

Fig. 1 presents a comprehensive workflow for detecting thresholds of ecosystem transition, consisting of four steps: model fitting, threshold detection, threshold significance validation, and cluster analysis. First, we fitted the relationships between 19 ecosystem variables and the ESI using both linear and nonlinear regression approaches. The nonlinear models included quadratic and generalized additive models (GAMs). For a GAM, we used the *gam()* function from the "mgcv" package (v4.2-1) in R, applying thin-plate splines for smoothing and setting the error distribution to Gaussian (family = "gaussian") [35]. The best-fitting models were selected based on the Akaike information criterion (AIC), with lower AIC values indicating a better fit (Table S3 online). All ecosystem variables exhibited a better fit with nonlinear models compared to linear model ($AIC_{nonlinear} < AIC_{linear}$). We then explored thresholds, as nonlinearity is a prerequisite for threshold detection. Second, we applied two types of threshold models to identify ecological thresholds: segmented regression (continuous change in slope) and stegmented regression (discontinuous change in both intercept and slope), following the definition of Berdugo et al. [7] (Fig. S4 online). In cases where GAM regression was the best-fitting model, segmented regression was used to indicate the point of maximum curvature. The most suitable threshold models (segmented/stegmented) were chosen using minimum AIC criteria, and their robustness was further validated with the Bayesian Information Criterion (BIC).

Third, we performed bootstraped linear regressions on both sides of each threshold for each variable 200 times. The Mann-Whitney U-test was used to compare the slopes before and after the threshold. All variables showed significant differences in the slopes on either side of the threshold (marked with an asterisk in Fig. 2c). Fourth, we applied the Elbow method and the Broken Stick method to determine the optimal number of clusters based on the within-cluster sum of squares [35] (Fig. S5 online). As the number of clusters increases, the within-cluster sum of squared errors decreases gradually. The "elbow point" where the curve levels off represents the optimal number of clusters, identifying four clusters. Accordingly, cluster analysis was employed to classify the 19 ecosystem variables into four groups, with corresponding ESI values of 1.0, 1.5, and 2.5, respectively. Ecosystems with an ESI value below 1.5 are categorized as "secure", with subdivisions into hyper-secure ecosystems (ESI < 1.0) and semi-secure ecosystems (1.0 ≤ ESI < 1.5). In contrast, ecosystems with ESI ≥ 1.5 are classified as "insecure" and further divided into light-insecure ecosystems (1.5 ≤ ESI < 2.5) and severe-insecure ecosystems (where ESI ≥ 2.5).

2.4. Structural equation modeling

The structural equation model (SEM) is an effective approach to elucidating the relationships among multiple variables. In this study, we constructed piecewise SEM (pSEM) to evaluate the direct and indirect effects of key ecosystem variables on species threat rates in both secure and insecure ecosystems. pSEM offers advantages over traditional SEM by enabling the simultaneous evaluation of multiple interrelated causal hypotheses while accommodating non-normal distributions commonly encountered in ecological data [36]. Moreover, constructing the pSEM model requires building a prior model based on existing knowledge.

To address spatial autocorrelation in the models, we incorporated simultaneous autoregressive models (SARs) into each pathway of the pSEM [37]. SARs account for spatial autocorrelation by utilizing neighborhood matrices that describe the relationships between the residuals at each location and those at neighboring locations [38]. Following the methodology outlined by García-Andrade et al. [37], we determined the appropriate spatial weights matrix for each pathway in the pSEM. Specifically, we fitted one ordinary least squares (OLS) model and six SARs models using two neighborhood distance matrices - minimum (d1) and maximum (d2) - with three weighting schemes: row standardized (W), globally standardized (C), and variance stabilizing (S). The best-fitting model for each pathway was selected based on the lowest Akaike Information Criterion (AIC) values and the highest R^2 values (Table S4 online). Consequently, in the final pSEM construction, we used the SARs model with the row-standardized spatial weight matrix (W) and the maximum neighborhood distance (d2), which minimized spatial autocorrelation in residuals as measured by Moran's I.

Before modeling, all predictor variables were standardized using the *scale()* function from the base package in R to ensure the comparability of coefficients. We calculated the correlation coefficients between the variables, ruling out the problem of multicollinearity ($R^2 < 0.8$) (Table S2 online). Besides, the influence of all predictor variables on species threat rates was assessed by considering spatial autocorrelation and calculating P-values using the *modified.ttest*() function from the "spatialpack" package in R [39]. Additionally, SARs models were fitted using the *nb2listw*(), *dnearneigh*(), and *knn2nb*() functions from the "spdep" package, and the *errorsarlm*() function from the "spatialreg" package [40]. The pSEM analyses were performed using the "piecewiseSEM" (version 2.3.0.1) package in R (version 4.4.1). Finally, the overall fit of the pSEM was evaluated using *Fisher's C* test, with stepwise model modifications made based on pathway significance ($P < 0.05$) and

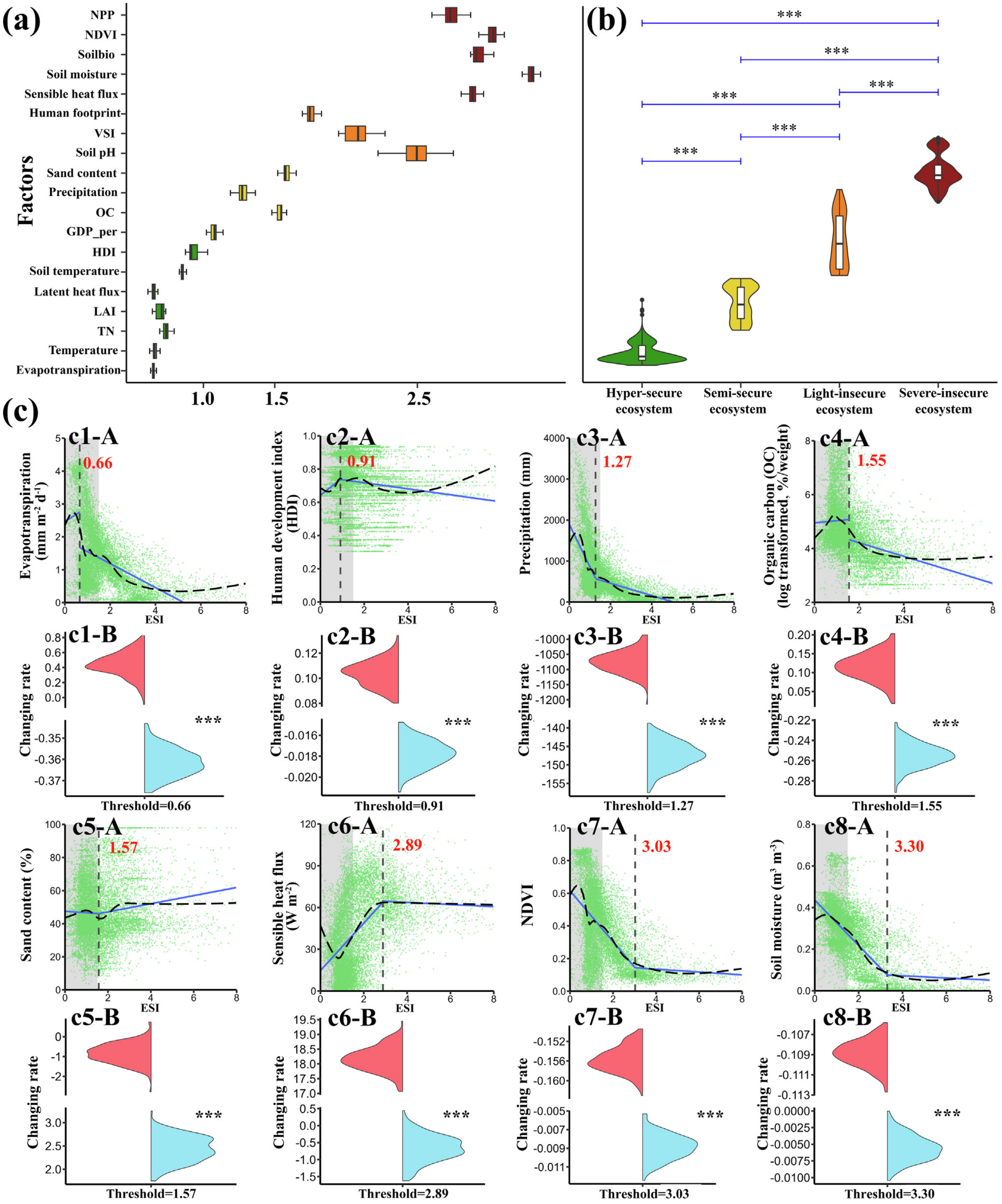

Fig. 2. (a) Identified thresholds and their bootstrapped confidence intervals. Each color represents a set of groups. Box plots display the median (solid line), interquartile range (upper and lower edges of the box), and the 10th to 90th percentiles (whiskers). (b) The cross-relationships among the four ecosystem security levels. (c) Nonlinear relationship between multiple ecosystem variables and ecological security index (ESI). Black dashed lines represent the smoothed trend fitted by a generalized additive model (GAM) and blue solid lines represent the linear fit at both sides of each threshold. Inserted red numbers and the vertical dashed lines denote the identified thresholds. Violin diagrams show the bootstrapped slopes at the threshold of the two regressions existing at each side of the threshold values (red: before the threshold; blue: after the threshold). Asterisks indicate significant differences when conducting a Mann-Whitney *U* test between before and after the threshold where: *** $P < 0.001$.

the goodness-of-fit of the model ($P > 0.05$). Following this, we analyzed the standardized coefficients for each pathway to interpret the influence of independent variables on dependent variables.

3. Results and discussion

3.1. Classification of ecosystem security levels

Our results demonstrate pervasive nonlinear relationships between multiple ecosystem variables and the ESI, indicating the existence of transition thresholds and classifying ecosystems into two distinct states: "secure" and "insecure", each with two levels per state (Fig. 2). Ecosystems with an ESI value below 1.5 are considered "secure", signifying strong ecological resilience, i.e., their ability to resist disturbances and maintain their original state [41]. In secure ecosystems, disturbances are primarily driven by climate change, as measured by changes in variables such as evapotranspiration, precipitation, and temperature (Fig. 2c1, c3, and Fig. S6 c10 online). However, higher precipitation and soil nutrients in these ecosystems directly support plant survival and growth (Fig. 2c4, c5, c8). The interaction between soil moisture and precipitation enhances water infiltration, regulates surface runoff, and facilitates groundwater recharge, all of which are crucial for terrestrial water cycles [42]. These favorable conditions promote healthy vegetation growth and maintain the ecosystem's energy balance. Furthermore, the process of plant transpiration, which releases water vapor into the atmosphere through leaf surfaces, reduces sensible heat flux and increases latent heat flux, leading to a cooling effect and slower warming [43,44]. These processes enable secure ecosystems to endure climate stress for a period through self-regulation and recovery mechanisms.

Ecosystems are classified as "insecure" with an ESI ≥ 1.5. Insecure ecosystems are characterized by significant declines in plant cover and productivity (Fig. 2c7 and Fig. S6 c19 online), which directly impair the ecosystems' ability to provide their essential functions and services. Furthermore, the transition to insecure ecosystems is marked by a shift in dominant vegetation types from forests to grasslands and shrublands (Fig. S9b online), accompanied by soil degradation characterized by nutrient-poor and sandy soils with lower soil water-holding capacity (Fig. 2c4, c5 online) [14]. This vegetation shift is ascribed to the deeper roots of shrubs, which can access stable water in deeper soil layers, along with a reduction in the overall sensitivity of vegetation to climatic fluctuations (Fig. S6c16 online) [45]. Additionally, plants adapt by developing smaller, thicker leaves and closing their stomata to minimize water evaporation in insecure ecosystems [1]. These adaptations weaken plant photosynthesis, the main source of oxygen production, thereby inhibiting plant growth and further destabilizing ecosystems.

The interactions between net oxygen production and hydrological (e.g., soil moisture and terrestrial water storage (TWS)) as well as thermal cycles (e.g., soil temperature and heat fluxes) also support this notion, as depicted in Fig. 3. Both soil moisture and TWS are closely associated with oxygen production (Fig. 3a–b), suggesting that regions with decreased net oxygen production experience a corresponding decline in the ecosystems' ability to store water. This reduction constrains plant growth and further decreases oxygen production, ultimately undermining ecosystems' ability to support life [46]. In addition, as net oxygen production increases, soil temperatures decrease due to higher transpiration rates, while sensible heat flux decreases and latent heat flux increases, contributing to temperature regulation (Fig. 3c–d). Conversely, decreases in net oxygen production are accompanied by rising temperatures, exacerbating thermal stress on the ecosystems. These feedback loops intensify net radiation and atmospheric dryness, accelerating soil moisture loss [47,48], thereby establishing a reinforcing cycle of warming and drying in insecure ecosystems (Fig. 3e).

3.2. Global distribution of ecosystems security levels

The identified thresholds were applied to categorize ecosystem security levels. Fig. 4 shows that the area of ecosystems considered hyper-secure accounts for only 26.6% of the global land area and is primarily distributed in South America, Siberia, Central Africa, and the Tibetan Plateau. In contrast, ecosystem areas considered insecure occupy 35.4% of the global land area, with 24.8% classified as light-insecure and 10.6% as severe-insecure. These insecure ecosystems are mainly located at the edge of deserts and are characterized by negative oxygen fluxes [49], increased aridity, and accelerated warming. Furthermore, figuring out how the future changes in ecosystem security levels is crucial. We used the ensemble means of the CMIP5 models (CMIP5-EM) to minimize uncertainties from inter-model variability. Our findings indicate that the spatial distributions and the area coverage of secure and insecure ecosystems predicted by CMIP5-EM are consistent with those indicated by observations (Fig. 4a–b and Fig. S7a online), demonstrating the reliability of CMIP5-EM for future projections. For a detailed discussion of the CMIP5-EM model, refer to Huang et al. [34].

By comparing the areal changes of insecure ecosystems from 2000–2015 to 2085–2100 under the RCP8.5 scenario, we found that the area percentages of semi-secure, light-insecure, and severe-insecure ecosystems are projected to increase by 5.2%, 7.3%, and 6.2%, respectively (Fig. 4d). In addition, the net area changes in hyper-secure and severe-insecure ecosystems are projected to be −3.8% and 5.3% of the global land area, respectively (Fig. S7b online). We also noticed that the increase in severe-insecure ecosystems is the most pronounced, reaching up to 15.9% of the global land area. By 2100, insecure ecosystems are projected to encompass 40.4% of the global land area under the RCP8.5 scenario.

3.3. Global distribution of threatened species and projected richness loss across ecosystems security levels

Ecosystem transition deteriorate habitat conditions and pose a threat to the survival of species. Fig. 5a–b illustrate the distribution of threatened rates for birds and mammals, calculated as the ratio of threatened species to total species (see Section 3 in Supplementary materials) across the four ecosystem security levels. It is clear that most threatened bird species are concentrated in the Sahara, West Asia, and India (Fig. 5a). Threatened bird species account for 22.8% and 16.6% in light-insecure and severe-insecure ecosystems, respectively. Furthermore, the situation for mammals is more severe, with a global average threatened rate of 4.3%, which is greater than that of 2.6% for birds. Specifically, the threatened rates for mammals in light-insecure and severe-insecure ecosystems are 17.3% and 11.9%, respectively (Fig. 5b). Additionally, regions with a higher number of threatened species often coincide with areas of high total species number (Fig. S8 online), particularly in biodiversity hotspots such as Southeast Asia and the Amazon [20]. We further projected species richness loss at the end of this century under the RCP4.5 and the RCP8.5 scenarios, based on the calculation of the net change in species richness relative to 1500 AD (see Section 4 in Supplementary materials) [23]. Our results indicate that the global average species richness loss is 17.2% under the RCP8.5 scenario, which is higher than 12.6% under the RCP4.5 scenario (Fig. 5c–d). Moreover, 14.3% of species richness

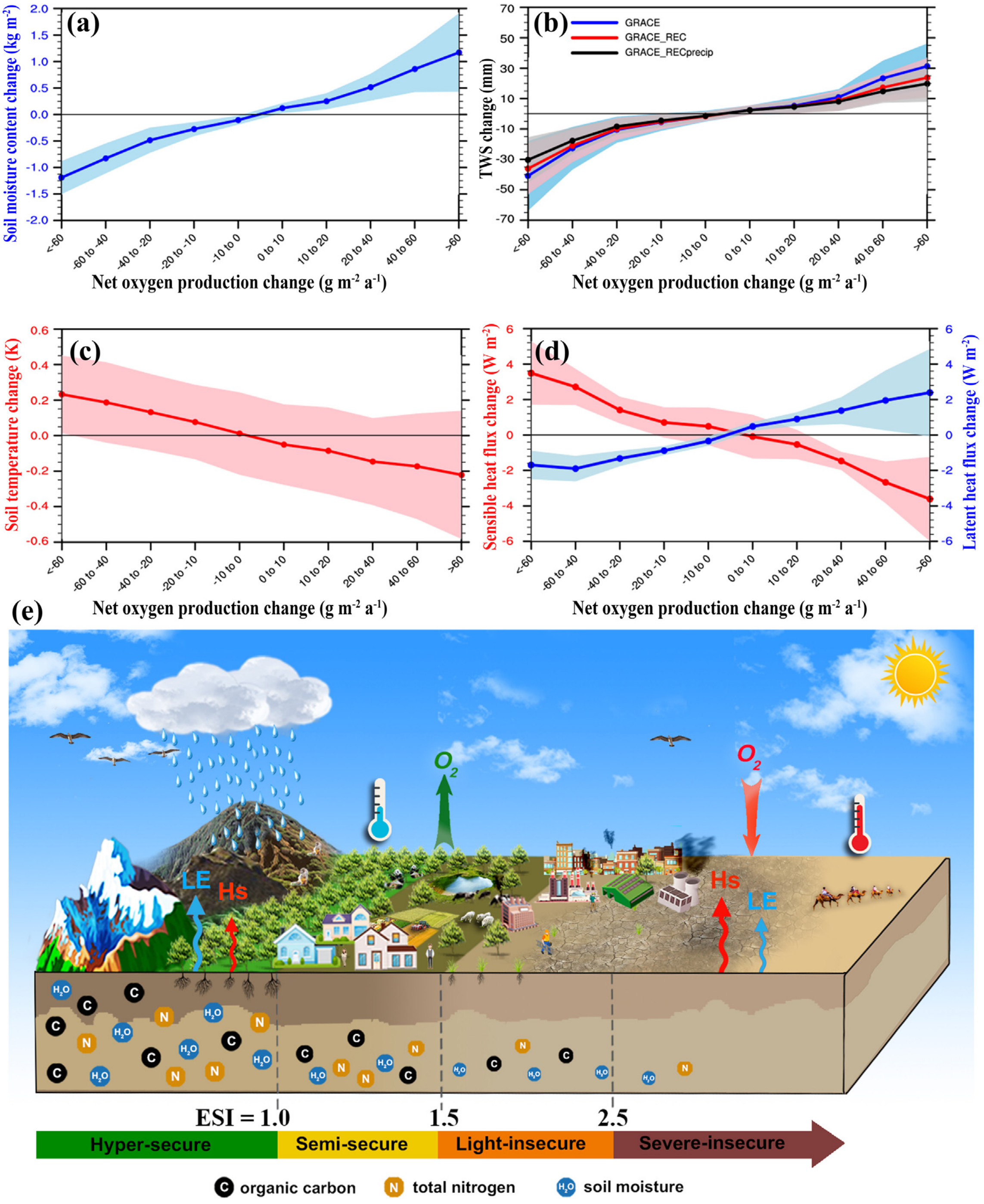

Fig. 3. The hydrological and thermal changes associated with net oxygen production change in terrestrial ecosystems. (a) The inter-annual variability in the regional average volumetric soil water within 60°S–60°N for 2000–2015 from the ERA5 dataset (blue line) with respect to the corresponding inter-annual variability in the net oxygen production derived from the MODIS dataset. (b) shows the terrestrial water storage (TWS) for 2002–2015 from GRACE satellite observations (blue line), and two statistical models of GRACE-REC (red line) and GRACE-RECprecip (black line) for 2000–2015 which are trained with GRACE observations. (c) Soil temperature (red line) for 2000–2015 from the ERA5 dataset. (d) Sensible heat flux (red, upward positive) and latent heat flux (blue, upward positive) for 2000–2015 from the ERA5 dataset. Shading denotes the ± 1 standard deviation range of the corresponding temporal variation. (e) A schematic diagram illustrates the characteristics of secure and insecure ecosystems. Green arrows denote O_2 production and red arrows denote O_2 consumption. LE, Hs, C, N, and H_2O represent the latent heat flux, sensible heat flux, soil organic carbon, soil total nitrogen, and soil moisture, respectively.

loss occurs in severe-insecure ecosystems, likely due to the inherently low species richness in these regions. Overall, insecure ecosystems contribute to 51.6% of the species richness loss under the RCP8.5 scenario, in contrast to 18.1% in hyper-secure ecosystems, underscoring the disproportionate impact of ecosystem transition on species richness loss.

3.4. Impact of ecosystem transition on threatened rates of birds and mammals

To better understand how ecosystem transition affect threatened species, we constructed a pSEM to investigate the direct and indirect influences of key ecosystem variables on threatened

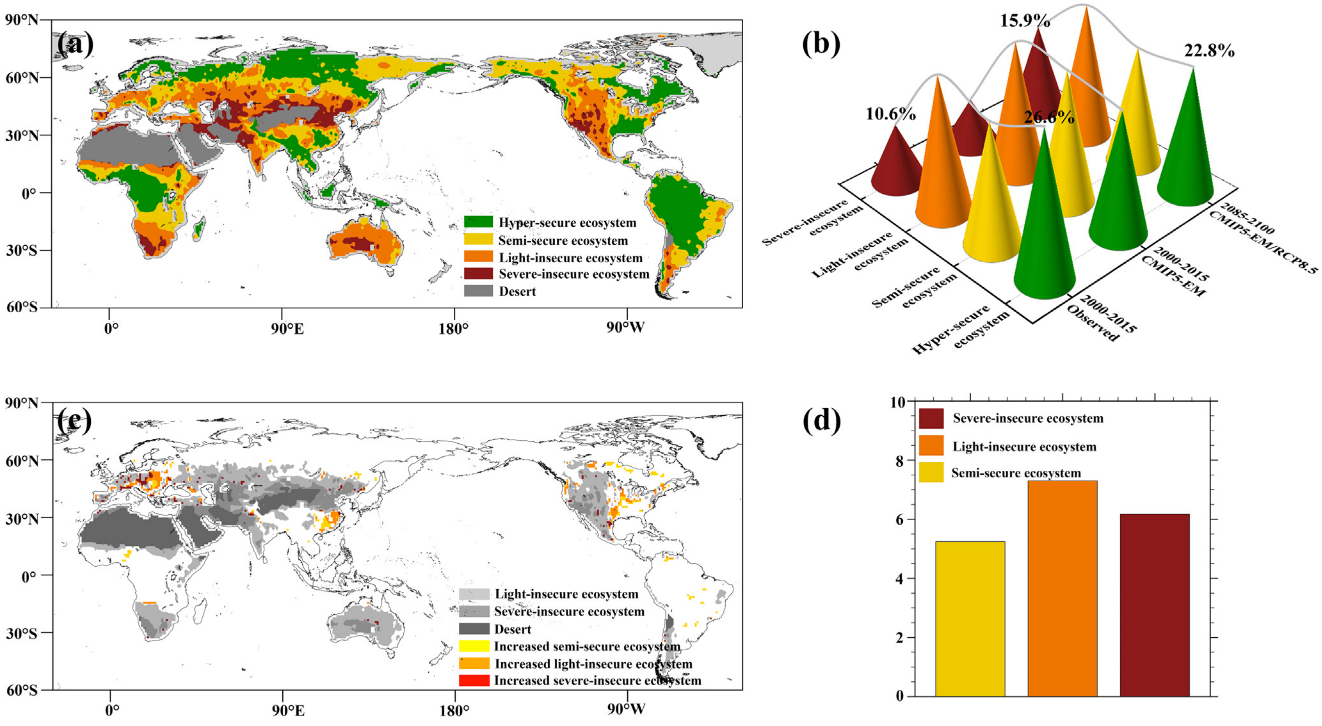

Fig. 4. (a) Spatial distribution of the four ecosystem security levels based on observed ESI values for 2000–2015. (b) Area coverage (percentage) of the four ecosystem security levels (60°S–60°N), based on observed ESI values for 2000–2015, CMIP5-EM ESI for 2000–2015, and CMIP5-EM ESI for 2085–2100. (c) The spatial distribution of projected changes in subtypes from the CMIP5-EM and the RCP8.5 scenario are shown relative to the baseline period (observations, 2000–2015) for 2085–2100. The gray shading denotes the baseline ecosystem security levels from 2000 to 2015. Changes include any shifts between adjacent and nonadjacent subtypes. For example, the "increased semi-secure" category represents regions that changed from being hyper-secure to semi-secure. (d) The increased area coverage (percentage) of the different ecosystem security levels is shown in (c).

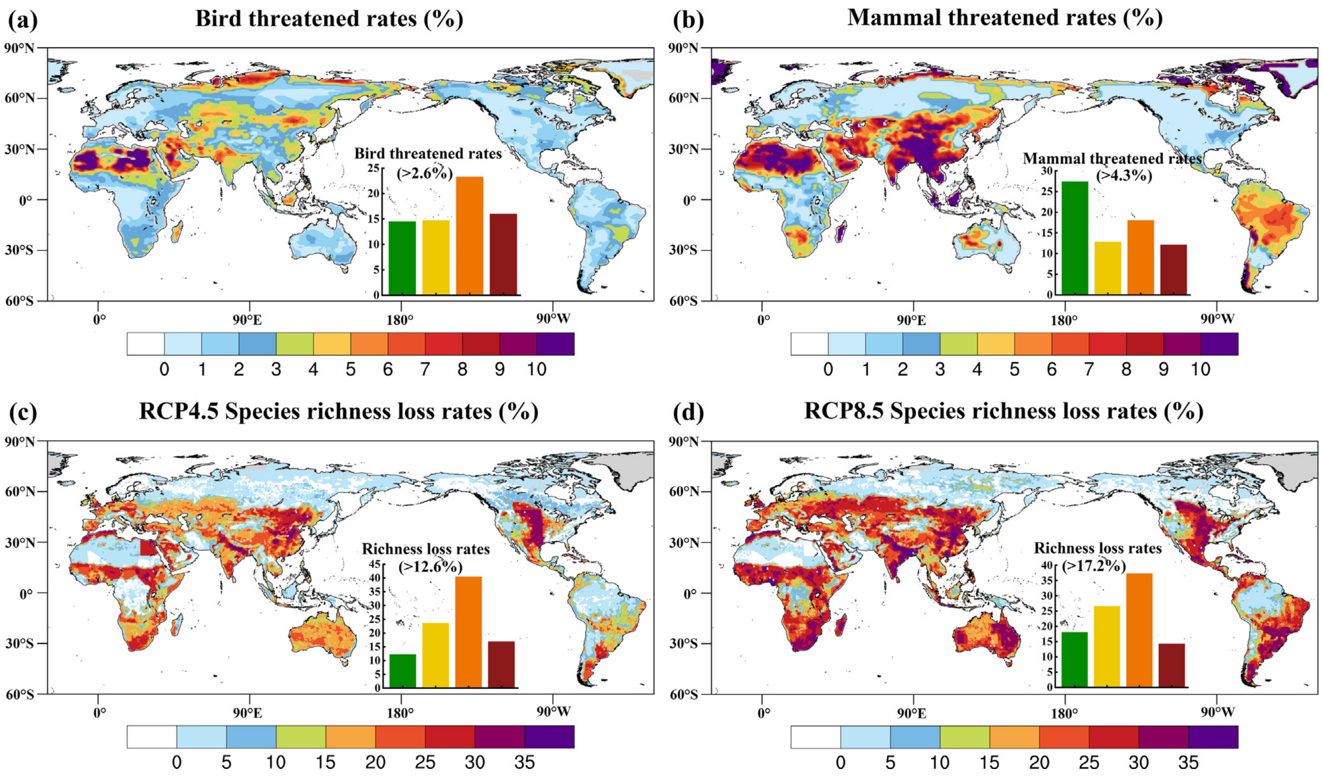

Fig. 5. Spatial distribution of threatened species rates for birds (a) and mammals (b). The threatened rate is calculated as the ratio of the number of threatened species (birds or mammals) to the number of total species (birds or mammals). The collection of data used here for birds and mammal species was up to 2013 and March 2018, respectively. Spatial distribution of species richness loss for total species by the end of this century under the RCP4.5 (c) and RCP8.5 (d) scenarios. The total species richness loss rate is calculated as the ratio of species to be lost relative to the total number of species. The inserted graphs show the threatened rates for birds and mammals, as well as species richness loss across four ecosystem security levels (60°S–60°N). (Four colors represent four levels of ecosystems, see Fig. 4a).

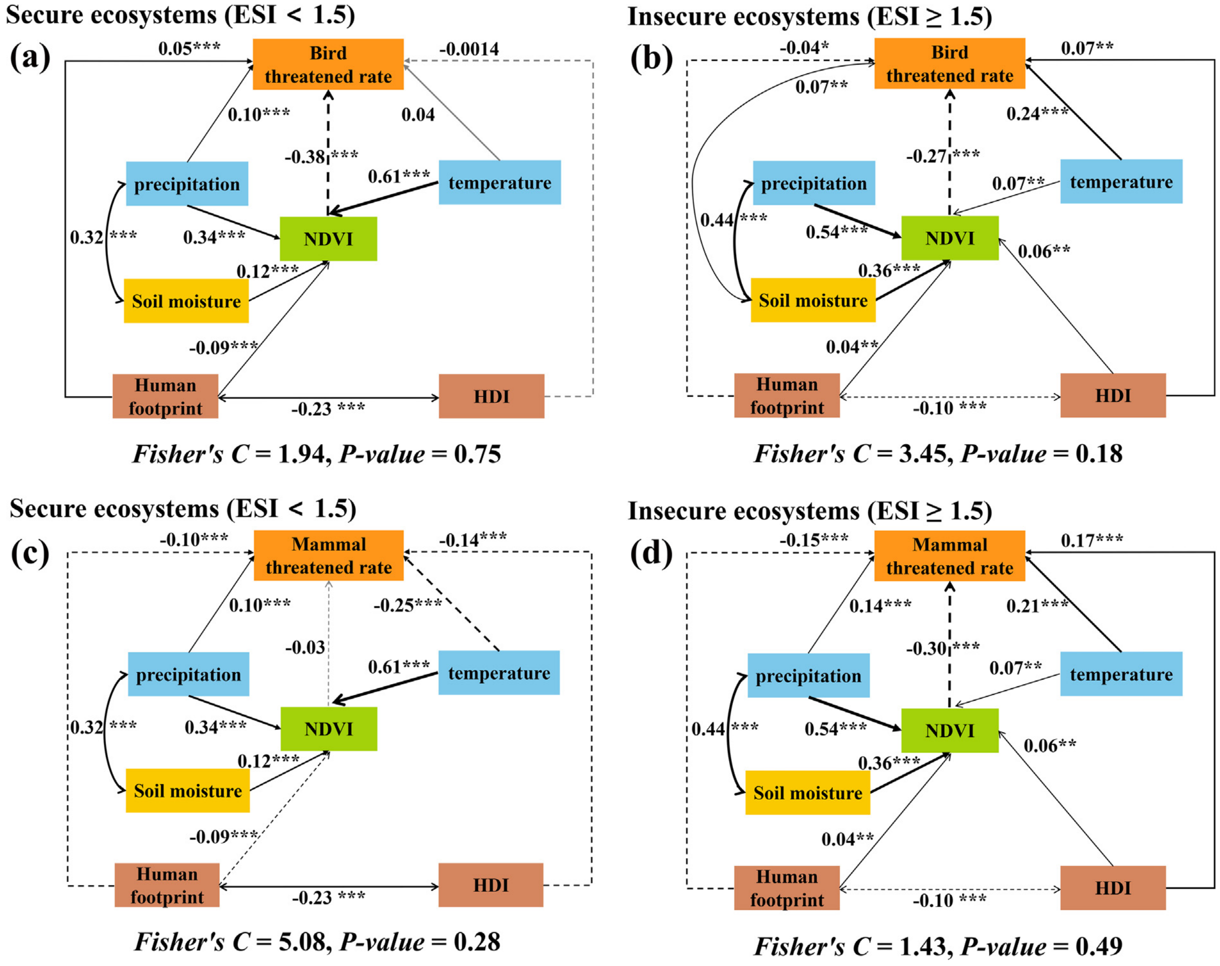

Fig. 6. Relationships between key ecosystem variables and species threatened rates. Piecewise structural equation models (pSEM) of birds (a, b) and mammals (c, d) threatened rates in secure and insecure ecosystems. Solid lines indicate positive paths, dashed lines indicate negative paths, and gray dotted lines indicate non-significant paths. The arrow width represents the size of path coefficients. The goodness-of-fit metrics of *P-value* > 0.05 indicate that the pSEM model is acceptable.

birds and mammals across secure and insecure ecosystems (Fig. 6). Key ecosystem variables were selected based on low correlations, while spatial autocorrelation was taken into consideration. The best-fitting pSEM indicates that NDVI (−0.38) has a strong negative effect on bird threatened rates in secure ecosystems, compared to a weaker effect (−0.27) in insecure ecosystems (Fig. 6a–b). This finding suggests that healthier vegetation is crucial for bird survival, as it provides nesting habitats, shelter, and essential food resources. In insecure ecosystems, however, the protective benefits of vegetation are diminished. The human footprint (0.05) shows a positive effect on bird threatened rates in secure ecosystems, implying that human activities such as land-use changes, deforestation, and habitat destruction increase the risk to bird populations [26,27]. In contrast, the human footprint (−0.04) has a negative effect in insecure ecosystems, potentially because the remaining bird species have evolved to tolerate certain levels of human disturbance.

Furthermore, the temperature variable (0.24) is a primary driver influencing bird threatened rates in insecure ecosystems. Rising temperatures destabilize the environmental conditions that birds depend on during critical periods, including breeding cycles and migration routes [50], placing additional pressure on vulnerable bird populations [25]. Climate disruption can cause mistimed migrations, which reduce reproductive success and contribute to population declines. Although some birds may adapt by seasonally migrating to less disturbed areas where they can establish new colonies, the success of this process depends on the implementation of effective conservation strategies. HDI (0.07) also exhibits a positive effect on bird threatened rates, indicating that regions with higher human development, characterized by increased industrialization, urbanization, and infrastructure expansion, face greater threats to bird populations [20], reflecting the socioeconomic drivers behind species threats. Additionally, climatic factors like precipitation and temperature indirectly influence bird threatened rates by positively impacting NDVI.

Regarding mammal threatened rates, NDVI (−0.03) does not significantly affect them in secure ecosystems, in contrast to its stronger impact on birds (Fig. 6a, c). However, NDVI (−0.30) exhibits a significant effect in insecure ecosystems (Fig. 6d). This is likely attributed to mammals' increased reliance on vegetation for shelter and protection from predators in environments with scarce hiding places [51]. Moreover, herbivores competing for dwindling resources may migrate in search of better habitats, while carnivores follow their prey, further intensifying the stress on mammals [52]. This trophic cascade amplifies pressures on mammal populations [53]. In addition, mammals struggle to adapt or migrate quickly enough during ecosystem transition, resulting in higher mortality [50]. Although colonization may occur in certain cases, it is constrained by geographical isolation or competition with native species. To enhance the survival chances of threatened species, it is essential to prioritize habitat connectivity and assist colonization efforts. As a result, these interactions reveal how threatened birds and mammals are impacted in secure and insecure ecosystems.

It should be noted that our study has certain limitations. First, while we integrated multiple ecosystem variables and employed threshold models to analyze ecosystem transition, other influential factors like food web disruptions and eutrophication were not fully accounted for in our analysis. Nevertheless, the threshold detection approach has been extensively applied in ecological studies and is regarded as robust [7,15,41]. Given the inherent uncertainty in the threshold of ecosystem transition, minor perturbations near the threshold can trigger a series of dramatic changes [9,54]. Second, our study provides valuable insights into how ecosystem transition threatens species richness loss, though it represents just one aspect of ecosystem dynamics. Future research should combine our findings with other ecological theories to better capture ecosystem responses to environmental stressors. Lastly, oxygen dynamics, shaped by photosynthesis and decomposition processes, require holistic consideration to understand their role within ecosystems.

4. Conclusion

Our study introduces the concept of ecosystem transition, emphasizing that species richness loss occurs abruptly as ecosystems shift from secure to insecure states. By analyzing the relationships between 19 ecosystem variables and the ESI, we identified critical thresholds that classify ecosystem security levels. Our projections suggest that by 2100, the ecosystem areas considered insecure will encompass 40.4% of the global land area under the RCP8.5 scenario, contributing to 51.6% of species richness loss. This finding reveals the disproportionate impact of insecure ecosystems on the decline of species richness, underscoring the heightened vulnerability of species to environmental degradation.

Thus, these insights remind us of the necessity to develop strategies aimed at preventing ecosystem transition, which is the prerequisite for mitigating species richness loss. Restoration and adaptation efforts should be targeted and tailored to specific ecosystem needs, with nature-based solutions offering a promising path to enhancing ecosystem resilience to climate change. In addition to the abrupt decline in species richness caused by ecosystem transition, the resulting adverse impacts on ecosystem functions and stability deserve further attention. Consequently, it is anticipated that our findings will stimulate research into the effects of two-way interactions between ecosystem transition and species richness loss.

Conflict of interest

The authors declare that they have no conflict of interest.

Acknowledgments

This work was jointly supported by the National Natural Science Foundation of China (41991231 and 42041004) and the Second Tibetan Plateau Scientific Expedition and Research Program (STEP)(2019QZKK0602), the China University Research Talents Recruitment Program (111 project, B13045). The authors acknowledge Tim Newbold for providing the species richness dataset. The authors also acknowledge the World Climate Research Programme's (WCRP) Working Group on Coupled Modelling (WGCM), the Global Organization for Earth System Science Portals (GO-ESSP) for producing the CMIP5 model simulations and making them available for analysis.

Author contributions

Jianping Huang designed the study. Li Fu contributed to data analysis, manuscript writing, and revisions. Guolong Zhang assisted with manuscript revisions. Yun Wei and Xiaoyue Liu analyzed the species data. All authors contributed to the discussion and interpretation of the results. All authors reviewed the manuscript.

Data availability

All data used in this study are publicly available and can be downloaded from the websites provided in the "Methods" section and Supplementary materials.

Appendix A. Supplementary material

Supplementary data to this article can be found online at https://doi.org/10.1016/j.scib.2025.03.001.

References

[1] Berdugo M, Vidiella B, Solé RV, et al. Ecological mechanisms underlying aridity thresholds in global drylands. Funct Ecol 2022;36:4–23.
[2] Armstrong McKay DI, Staal A, Abrams JF, et al. Exceeding 1.5°C global warming could trigger multiple climate tipping points. Science 2022;377:eabn7950.
[3] Lenton TM, Rockström J, Gaffney O, et al. Climate tipping points — too risky to bet against. Nature 2019;575:592–5.
[4] Wang J, Yan R, Wu G, et al. Unprecedented decline in photosynthesis caused by summer 2022 record-breaking compound drought-heatwave over Yangtze River Basin. Sci Bull 2023;68:2160–3.
[5] Liu X, Huang J, Huang J, et al. Estimation of gridded atmospheric oxygen consumption from 1975 to 2018. J Meteorol Res 2020;34:646–58.
[6] An L, Wang J, Huang J, et al. Divergent causes of terrestrial water storage decline between drylands and humid regions globally. Geophys Res Lett 2021;48:e2021GL095035.
[7] Berdugo M, Delgado-Baquerizo M, Soliveres S, et al. Global ecosystem thresholds driven by aridity. Science 2020;367:787–90.
[8] Scheffer M, Carpenter S, Foley JA, et al. Catastrophic shifts in ecosystems. Nature 2001;413:591–6.
[9] van Nes EH, Arani BM, Staal A, et al. What do you mean, 'tipping point'? Trends Ecol Evol 2016;31:902–4.
[10] Scheffer M, Carpenter SR, Lenton TM, et al. Anticipating critical transitions. Science 2012;338:344–8.
[11] Suding KN, Gross KL, Houseman GR. Alternative states and positive feedbacks in restoration ecology. Trends Ecol Evol 2004;19:46–53.
[12] Johnston ASA, Meade A, Ardö J, et al. Temperature thresholds of ecosystem respiration at a global scale. Nat Ecol Evol 2021;5:487–94.
[13] Niu S, Chen W, Liáng LL, et al. Temperature responses of ecosystem respiration. Nat Rev Earth Environ 2024;5:559–71.
[14] Fu Z, Ciais P, Feldman AF, et al. Critical soil moisture thresholds of plant water stress in terrestrial ecosystems. Sci Adv 2022;8:eabq7827.
[15] Zhang J, Feng Y, Maestre FT, et al. Water availability creates global thresholds in multidimensional soil biodiversity and functions. Nat Ecol Evol 2023;7:1002–11.
[16] Wang C, Wang X, Liu D, et al. Aridity threshold in controlling ecosystem nitrogen cycling in arid and semi-arid grasslands. Nat Commun 2014;5:4799.
[17] Scheffer M, Hirota M, Holmgren M, et al. Thresholds for boreal biome transitions. Proc Natl Acad Sci USA 2012;109:21384–9.
[18] Hirota M, Holmgren M, Van Nes EH, et al. Global resilience of tropical forest and savanna to critical transitions. Science 2011;334:232–5.
[19] Dirzo R, Raven PH. Global state of biodiversity and loss. Annu Rev Environ Resour 2003;28:137–67.
[20] Ceballos G, Ehrlich PR, Barnosky AD, et al. Accelerated modern human–induced species losses: entering the sixth mass extinction. Sci Adv 2015;1:e1400253.
[21] Almond REA, Grooten M, Juffe Bignoli D, et al. Living Planet Report 2022 – Building a nature-positive society. WWF 2022.
[22] Urban MC. Accelerating extinction risk from climate change. Science 2015;348:571–3.
[23] Newbold T, Hudson LN, Hill SLL, et al. Global effects of land use on local terrestrial biodiversity. Nature 2015;520:45–50.
[24] Jung M, Rowhani P, Scharlemann JPW. Impacts of past abrupt land change on local biodiversity globally. Nat Commun 2019;10:5474.
[25] Powers RP, Jetz W. Global habitat loss and extinction risk of terrestrial vertebrates under future land-use-change scenarios. Nat Clim Change 2019;9:323–9.

[26] Tilman D, Clark M, Williams DR, et al. Future threats to biodiversity and pathways to their prevention. Nature 2017;546:73–81.

[27] Maxwell SL, Fuller RA, Brooks TM, et al. Biodiversity: the ravages of guns, nets and bulldozers. Nature 2016;536:143–5.

[28] Pörtner H-O, Scholes RJ, Agard J, et al. IPBES-IPCC co-sponsored workshop report on biodiversity and climate change. IPBES 2021.

[29] Barnosky AD, Matzke N, Tomiya S, et al. Has the Earth's sixth mass extinction already arrived? Nature 2011;471:51–7.

[30] Li C, Fu B, Wang S, et al. Climate-driven ecological thresholds in China's drylands modulated by grazing. Nat Sustain 2023;6:1363–72.

[31] Delgado-Baquerizo M, Maestre FT, Gallardo A, et al. Decoupling of soil nutrient cycles as a function of aridity in global drylands. Nature 2013;502:672–6.

[32] Jenkins CN, Pimm SL, Joppa LN. Global patterns of terrestrial vertebrate diversity and conservation. Proc Natl Acad Sci USA 2013;110:E2602–10.

[33] Huang J, Liu X, He Y, et al. The oxygen cycle and a habitable Earth. Sci China Earth Sci 2021;64:511–28.

[34] Huang J, Yu H, Han D, et al. Declines in global ecological security under climate change. Ecol Indic 2020;117:106651.

[35] Team RC. R: a language and environment for statistical computing. R Foundation for Statistical Computing 2020.

[36] Lefcheck JS. piecewiseSEM: piecewise structural equation modelling in R for ecology, evolution, and systematics. Methods Ecol Evol 2016;7:573–9.

[37] García-Andrade AB, Carvajal-Quintero JD, Tedesco PA, et al. Evolutionary and environmental drivers of species richness in poeciliid fishes across the Americas. Global Ecol Biogeogr 2021;30:1245–57.

[38] Dormann CF, McPherson JM, Araújo MB, et al. Methods to account for spatial autocorrelation in the analysis of species distributional data: a review. Ecography 2007;30:609–28.

[39] Vallejos R, Osorio F, Bevilacqua M. Spatial relationships between two georeferenced variables: with applications in R. Heidelberg: Springer; 2020.

[40] Bivand RS, Pebesma EJ, Gómez-Rubio V, et al. Applied spatial data analysis with R. Heidelberg: Springer; 2008.

[41] Ingrisch J, Umlauf N, Bahn M. Functional thresholds alter the relationship of plant resistance and recovery to drought. Ecology 2023;104:e3907.

[42] Sehler R, Li J, Reager J, et al. Investigating relationship between soil moisture and precipitation globally using remote sensing observations. J Contemp Water Res Educ 2019;168:106–18.

[43] Huang J, Yu H, Dai A, et al. Drylands face potential threat under 2°C global warming target. Nat Clim Change 2017;7:417–22.

[44] Huang J, Yu H, Guan X, et al. Accelerated dryland expansion under climate change. Nat Clim Change 2016;6:166–71.

[45] Seddon AWR, Macias-Fauria M, Long PR, et al. Sensitivity of global terrestrial ecosystems to climate variability. Nature 2016;531:229–32.

[46] Liu Q, Guo H, Zhang J, et al. Global assessment of terrestrial productivity in response to water stress. Sci Bull 2024;69:2352–6.

[47] Seneviratne SI, Corti T, Davin EL, et al. Investigating soil moisture–climate interactions in a changing climate: a review. Earth Sci Rev 2010;99:125–61.

[48] Sherwood S, Fu Q. A drier future? Science 2014;343:737–9.

[49] Ding L, Huang J, Li C, et al. Variations in terrestrial oxygen sources under climate change. Sci China Earth Sci 2022;65:1810–23.

[50] Wilcove DS, Wikelski M. Going, going, gone: is animal migration disappearing. PLoS Biol 2008;6:e188.

[51] Benitez-Lopez A, Alkemade R, Schipper A, et al. The impact of hunting on tropical mammal and bird populations. Science 2017;356:180–3.

[52] Ripple WJ, Estes JA, Beschta RL, et al. Status and ecological effects of the world's largest carnivores. Science 2014;343:1241484.

[53] Estes JA, Terborgh J, Brashares JS, et al. Trophic downgrading of planet Earth. Science 2011;333:301–6.

[54] Scheffer M, Bascompte J, Brock WA, et al. Early-warning signals for critical transitions. Nature 2009;461:53–9.